ELSEVIER

Coordination Chemistry Reviews
216–217 (2001) 333–361

COORDINATION CHEMISTRY REVIEWS

www.elsevier.com/locate/ccr

ICCC34 — golden edition of coordination chemistry reviews. Coordination chemistry for the neurosciences

Shawn C. Burdette, Stephen J. Lippard *

Department of Chemistry, Massachusetts Institute of Technology, 77 Massachusetts Avenue, Cambridge, MA 02139, USA

Received 8 August 2000; accepted 19 December 2000

Contents

* Corresponding author. Tel.: +1-617-2531892; fax: +1-617-2588150.
E-mail address: lippard@lippard.mit.edu (S.J. Lippard).

PII: S0010-8545(01)00308-3

Abstract

Metal ions are integral components of numerous enzymes and proteins. Although the field of bioinorganic chemistry has not focused on the brain and central nervous system, metal ions are vital to many neurological functions and are implicated in several neurological disorders. In this review, we give a brief overview of the functions of metal ions in neurobiology and the highlight recent advances and uses of fluorescent sensors to study the neurotransmitters nitric oxide and zinc. Emphasis is placed on work from our laboratory to devise sensors for NO and Zn^{2+}, a project that was initiated 3 years ago in a continuing effort to study the inorganic chemistry of the nervous system.

Keywords: Bioinorganic chemistry; Metal ions; Nervous system

1. Bioinorganic chemistry at the beginning of the 21st century

At the close of the 20th century, the fundamental importance of metal ions in biology was clearly established after more than 50 years of extensive research [1–5]. Important developments in enzymology allowed metalloproteins to be expressed and studied by site directed mutagenesis. Technological advances in magnetic and electronic spectroscopy facilitated exploration of the properties of metal active sites. And innovative techniques in macromolecular crystallography afforded atomic resolution structures of numerous metalloenzymes [6]. In addition to their functions in proteins and enzymes, metals have emerged as important therapeutic and diagnostic agents in medicinal chemistry [7,8]. New metalloenzymes continue to be discovered with novel functions and properties, and there is an increase in the number of metal ions being evaluated as remedies for human ailments [9–11].

The last 50 years has also witnessed the use of small molecule model compounds as important tools for exploring the properties of systems that are difficult to study in their natural state [12]. Reactive enzyme intermediates, as well as systems where detailed structural information is not available, can often be characterized only with the aid chemical models. Model studies can provide information to help direct work on the natural enzymes.

Of the areas at the interface between inorganic chemistry and biology that remain to be explored, the role of metal ions in neuroscience is perhaps the most prominent. Bioinorganic chemists have been attracted historically to systems involving transition metal ions because of their valuable magnetic and spectroscopic properties. Despite the preponderance of Na^+, K^+, Mg^{2+} and Ca^{2+} in biological processes, the inorganic chemistry community has often ignored these metal ions because they lack the electronic and magnetic properties of their d-block counterparts [11]. In a similar manner, neuroscientists have focused on Group 1 and 2 metal ions and, until recently, have dismissed transition metals such as Mn, Fe, Cu, and Zn as inconsequential trace elements in the central nervous system [13]. By combining the ability of bioinorganic chemists to evaluate the properties of metal

ions with that of neuroscientists to explore the physiology of the nervous system, a powerful new alliance could emerge for understanding such complex processes as neurotransmission and synaptic plasticity. An important consequence would be to uncover the causes of, and develop treatments for, neurodegenerative disease.

2. Inorganic chemistry and neurosciences

The nervous system is a complex electrochemical computer linked to mechanical components. The extracellular medium that envelops nerve cells and the cytoplasm of these cells are replete with inorganic ions that help generate electrical currents required for movement, sensation, reflexes, learning, and memory. The unequal distribution of ions across cell membranes, and the differential permeability of these ions produced by pumps and channels, generates membrane potentials that provide the driving force for neurological events [14]. The primary ions involved in the generation and regulation of the electric currents are the s-block alkali and alkaline earth metals Na^+, K^+, Mg^{2+} and Ca^{2+}. The primary intracellular ion is K^+, and Na^+ is the major cation outside the cell. The approximate concentrations of these ions are summarized in Table 1.

Recently our laboratory has initiated three projects in the neurosciences. One is to prepare structural and functional models for the K^+ channel and the other two are to explore the neurological functions of ionic zinc (Zn^{2+}) and nitric oxide (NO) by preparing new fluorescent sensors and applying them to biological systems. This review highlights recent advances in these areas with a focus on our progress in the synthesis and application of Zn^{2+} and NO fluorescent sensors over the past 3 years. We also provide a brief overview of inorganic chemistry relevant to the brain and nervous system, as well as a perspective on our future goals including work on ion channel modeling.

2.1. The chemistry of s-block metal ions and the K^+ channel

Cursory examination of the physical and chemical properties of Na^+ and K^+ reveals that the two ions are quite similar. Both are closed shell, hard ions that prefer oxygen donors; they have identical coordination geometries and display similar exchange kinetics for bound water molecules [1]. Despite these similarities, ion channels, a class of transmembrane proteins responsible for a host of biological events, can discriminate between Na^+ and K^+ ions with unprecedented selectivity.

Table 1
Concentrations (mM) of important metal ions in cells [1,5]

Cation	K^+	Na^+	Ca^{2+}	Mg^{2+}
Internal	155	12	$<10^{-7}$	30
External	4	145	1.5	1

In addition to this selective binding property, channels facilitate the flow of ions at a rate near the diffusion limit. Perhaps the most significant recent breakthrough in understanding metal ion discrimination and ion channel function was the determination in 1998 of the X-ray crystal structure at 3.2 Å resolution of the KcsA K^+ channel [15].

The structural information provided by the crystal structure affords considerable insight into the mechanism by which the potassium channel discriminates for K^+ over Na^+ by a factor of 10^3–10^4 and passes current at a rate of 10^8 ions s^{-1} [16,17]. The channel is a C_4-symmetric tetramer having a pore created at the interface of the four subunits. The key event in ion discrimination takes place at the extracellular end of the pore in a region termed the selectivity filter, a narrow passageway formed by the confluence of 12–16 oxygen atoms, contributed primarily from protein backbone carbonyl groups. An equatorial belt of four water molecules around an octahedral K^+ ion is stripped away and perfectly compensated by four peptide backbone carbonyl oxygen atoms as potassium passes through the filter. For the smaller Na^+ ion, only three such water molecules can be so compensated. The fourth water thus provides a steric block to passage of the partially hydrated sodium ion through the filter. Two octahedrally coordinated ions were located within the selectivity filter in the crystal structure analysis. Each was assumed to be equatorially coordinated by four oxygen atoms from the protein and two axial water molecules. A third hydrated ion appears at the intracellular side of the channel, presumably awaiting entry into the filter region. In the absence of excess K^+ ions, the filter has an affinity for K^+ of ~ 3 μM, but this value is altered to ~ 0.1 M in the presence of other K^+ ions [17]. This dramatic difference illustrates how the protein balances the needs for selectivity and speed. At physiological concentrations, the channel contains several ions that diminish the inherent affinity for K^+. In addition to the two ions that are held in the pore by chemical bonds, the third uncoordinated K^+ in the selectivity filter is presumably stabilized by protein electrostatics. The alignment of four helix dipoles acts as a stabilizing force for the third ion in the lipophilic membrane [15]. The perfect positioning of these three K^+ ions allows coordination chemistry and electrostatic repulsion to work in concert permitting selectivity at high flow rates.

The K^+ channel structure provides a conspicuous example of the importance of metal ion coordination chemistry in controlling the selection of metal ions and determining their role in molecular neurobiology. Other work includes studies of the Na^+–K^+ pump [18], of Ca^{2+} pumps [19], and of the relationships between ion channels and neurological disease [20,21]. The potential for growth of this field is enormous. Despite the wealth of opportunities, bioinorganic chemists have yet to make a significant contribution.

2.2. Transition metals including zinc in the brain

The quantities of Fe, Zn, and Cu present in the brain are significantly lower than that of K^+ and Na^+, but similar to the concentration of Mg^{2+}, which is present at 0.1–0.5 mM [13]. Recent work suggests that redox active metals including Mn

generate and/or protect cells from dioxygen and protein radicals that are implicated in neurological disease. The dual capacity of transition metals both to regulate and to generate detrimental radicals requires that their homeostasis be tightly controlled [4,22–25].

Iron is involved in the synthesis of neurotransmitters [26], required as a cofactor in brain energy metabolism [25] and suspected to play a role in neural communication. Copper enzymes also participate in several important neurochemical processes. Included are peptidylglycine α-amidating monooxygenase that modifies neuropeptides, lysyl oxidase that cross-links elastin and collagen, and Cu,Zn-superoxide dismutase (SOD) that disproportionates harmful superoxide radicals [27]. Although studies of the chaperone protein (CCS) for providing copper to superoxide dismutase suggest that there is essentially no free Cu^{2+} in the cytoplasm [28], there is a significant possibility that bound Cu^{2+} in neurons and glia, the two major cell types in brain, can be labilized and become cytotoxic. There may be a function for released Cu^{2+} during neurotransmission, but so far it has been difficult to establish such a role [13]. The current interest in learning how metal ions are transported to their target proteins [25,29], and the increase in research implicating metals in Alzheimer's disease (AD), Parkinson's disease (PD), amyotrophic lateral sclerosis (ALS), and aging, indicate the need for bioinorganic chemists to help unravel the roles metal ions in neuroscience [13,30,31].

Although not redox-active like Fe, Cu, and other first row transition metals required for neurobiology, Zn^{2+} also plays an important role in the central nervous system (CNS) [32–34]. Whereas most Zn^{2+} in the CNS is tightly bound to proteins and enzymes, pools of free Zn^{2+} occur at high levels in the mossy fiber terminals of the hippocampus [35]. Zinc ion has the ability to modulate a variety of ion channels [36], may play a role in neuronal death during seizures [37], is involved in neurodegenerative disorders [38], and may be vital to neurotransmission [39]. Since many of the effects of Zn^{2+} have been demonstrated in vitro by the addition of the exogenous metal ion, it is important to devise methods for interrogating how it functions under physiological conditions [32,35].

Concentrations of ionic Zn^{2+} are estimated to vary widely throughout the CNS. The levels of Zn^{2+} in the brain and elsewhere are regulated by three homologous Zn^{2+} transport proteins (ZnT-1, ZnT-2, and ZnT-3) [40–42] and by metallothioneins (MTs) [43–45], including MT-III and MT-IV, which are expressed mainly in the brain [46–49]. In addition, Zn^{2+} can be released from synaptic vesicles [35,50] and can enter postsynaptic cells through voltage-dependent Ca^{2+} channels [32,51]. Because of its diverse functions, Zn^{2+} continues to be an interesting subject of research in neurobiology.

2.3. Neurochemistry of NO and other RNOS

Nitric oxide (NO) became the focus of many biological studies following the discovery of its role as a signaling agent in the cardiovascular system [52], nervous system [53], and brain [54]. The three isozymes of nitric oxide synthase (NOS) catalyze the biosynthesis of NO and L-citrulline from dioxygen and L-arginine.

Neuronal NOS (nNOS), which is expressed in postsynaptic terminals of neurons in the brain, and endothelial NOS (eNOS), which is found in endothelial cells lining blood vessels, are activated by the binding of calmodulin at elevated levels of intracellular Ca^{2+} [55]. Agonists like acetylcholine and glutamate generate increased levels of Ca^{2+} that induce these two NOS enzymes to release small amounts of NO [56]. Inducible NOS, which is regulated at the level of transcription [57], is expressed by macrophages and produces higher levels of NO over longer periods of time. Once formed under physiological conditions, NO can have a lifetime up to 10 min [58] and can diffuse over a range of 100–200 μm [59]. The relatively long lifetime and dispersion range permit NO to react with a variety of targets. Reaction with O_2 forms reactive nitric oxide species (RNOS) such as NO_2 and NO^+, and with superoxide ($O_2^{\bullet -}$), peroxynitrite ($ONOO^-$), a potent oxidant, arises. In addition to reactions with oxygen species, NO can react with thiols, amines, and transition metal centers such as iron in oxyhemoglobin [60]. Although certain of these reactions may be fairly innocuous, peroxynitrite appears to be the main culprit involved in nitration of tyrosine residues found in disease states, and can cause DNA strand breaks [61].

Over the past decade several possible roles for NO and RNOS in biological systems have been explored. NO activates soluble guanylyl cyclase, which catalyzes the formation of the intracellular messenger guanosine 3′,5′-monophosphate, and NO is proposed to act as a retrograde neurotransmitter in the hippocampus during memory formation [62]. In addition, NO damages DNA and inhibits its repair [63,64]. It is also implicated in vasodilation [65], neurotoxicity [66], and neurotransmission [57,62]. Although NO is necessary for many neurological signaling functions, its overproduction appears to be responsible for oxidative damage in the CNS. NO and RNOS species are suspected to play major roles in the pathogenesis of several neurological disorders, such as AD, ALS, PD, multiple sclerosis (MS), Huntington's disease (HD), and stroke [56,66].

The study of the various functions of NO in biological systems is often hampered by the lack of a method to detect it directly and to provide temporal and spatial information about its distribution. Fluorescent sensors are ideally suited tools for performing these types of measurements [67,68]. The development of an array of fluorescent sensors for Ca^{2+} has facilitated the study and understanding of its functions in the cell [69–75]; however, few sensors exist for directly imaging NO.

3. Fluorescent sensors for NO and RNOS

The stringent criteria required for an effective intracellular fluorescent sensor for detecting analytes, particularly an inorganic radical like NO, create design challenges. Sensors must be able to bind selectively and reversibly the species of interest in the presence of competitors that could produce a false signal, and should have an affinity (K_d) close to the median concentration of the analyte. The sensor should produce a positive fluorescence response or a significant change in the excitation or emission maximum upon binding of the analyte. The reporting group of the sensor

should have an intense fluorescence with an excitation maximum above 340 nm to facilitate use with glass microscope lenses and to avoid UV-induced cell damage. An emission wavelength exceeding 500 nm helps to prevent interference by autofluorescence from native species in the cell. In addition to its spectral properties, the sensor must be water-soluble and have the ability to be passively and irreversibly loaded into cells. Selective binding of NO in the presence of O_2 presents a challenge, and NO is known to quench the fluorescence of fluorophores [76,77].

3.1. Griess assay, microsensors and fiber optic sensors

Several approaches to detecting biological NO are available that do not involve a fluorescent signal, including the Griess assay that measures nitrite [78], and electrochemical microsensors [79–81]. These methods and others are invaluable in studying NO biochemistry, but are often limited in sensitivity and ability to provide spatial information [82,83]. Fiber optic fluorescent sensors based on soluble guanylate cyclase (sGC) [84], cytochrome *c′* [84,85], vitamin B12 [86], and 4-carboxy-2′-7′-difluorofluorescein succinimidyl ester adsorbed on a gold surface [87] are capable of directly detecting NO, but can only measure NO localized near the tip of the fiber optic. Small molecule fluorescent sensors seem to provide the most powerful approach for detecting intracellular NO.

3.2. FNOCTs

Fluorescent sensors for directly detecting NO evolved from a class of *o*-quinodimethanes developed for monitoring NO by EPR spectroscopy [88–90]. The sensors called fluorescent nitric oxide cheletropic traps (FNOCTs, Scheme 1) incorporate a phenanthrene fluorophore into a *o*-quinodimethane scaffold. Reaction of **1** with nitric oxide generates the nitroxide radical **2** which can be reduced to the corresponding hydroxylamine, **3**. The dimethylamino group was incorporated into **1b** to induce a red shift in the excitation and emission wavelengths compared to **1a**. Reaction of NO with FNOCT **1b** produces an approximately ninefold fluorescence increase ($\Phi_{\mathbf{1b}} = 0.03$, $\Phi_{\mathbf{3b}} = 0.27$) in the presence of ascorbate as a

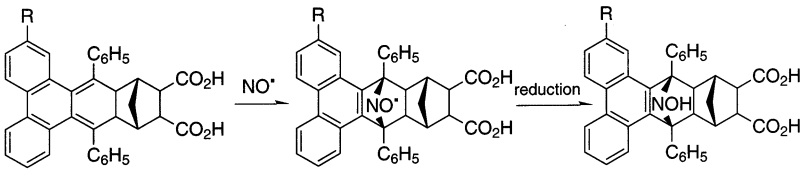

1 Non-fluorescent

2 Weakly fluorescent

3 Fluorescent

1a, 2a, 3a R = H
1b, 2b, 3b R = $N(CH_3)_2$

Scheme 1.

reductant. Compound **1b** has optical properties amenable for intracellular applications ($\lambda_{ex} = 460$ nm, $\lambda_{em} = 600$ nm), and can detect NO at nM concentrations. The ability of FNOCT to detect biological NO was demonstrated in alveolar macrophages after functionalization of the carboxylic acids with acetoxymethylesters to permit cell loading. Although FNOCTs are capable of detecting intracellular NO, they also react with peroxynitrite. In addition, the second-order rate constant (100 M^{-1} s^{-1}) of FNOCTs reaction with NO is slower than the reaction of NO with superoxide and iron complexes [90]. FNOCTs also require a reductant to achieve maximum quantum yields, which may limit their use for certain applications. FNOCTs will soon become available to the biological community at large [91].

3.3. DAFs

The most widely used fluorescent probes for indirectly detecting intracellular NO are diaminofluoresceins (DAFs) [92,93]. DAFs were developed as NO sensors to overcome problems experienced using diaminonaphthalenes at physiological conditions [94,95]. Under aerobic conditions, DAFs react with NO at concentrations as low as 3 nM to form triazolofluoresceins (DAF-Ts, Scheme 2). Eleven variations of DAFs have been examined including the more stable *N*-methylated derivatives and a fluorinated derivative that has superior pH properties. The diamino compounds have low quantum yields ($\Phi_{DAF} = 0.002–0.007$), presumably resulting from intramolecular PET (photoinduced electron transfer) quenching of the excited state by the free amines, which increase dramatically upon the formation of the triazole ring ($\Phi_{DAF-T} = 0.53–0.92$). DAFs can be loaded into cells by esterification of the phenols for detection of intracellular NO. Recently similar fluorescent probes based on rhodamine chromophores have been prepared [96]. Despite their excellent optical properties owing to the use of fluorescein and rhodamine fluorophores, DAFs react with NO^+ equivalents such as nitric anhydride (N_2O_3) instead of directly with NO, so conclusions about NO based experimental results can be somewhat ambiguous.

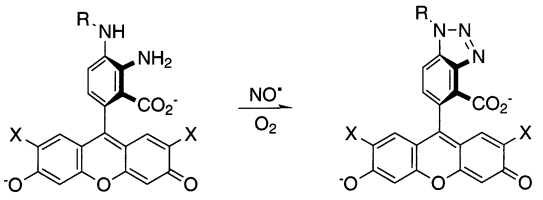

Non-fluorescent Fluorescent

DAF-1 (**4**) X, R = H
DAF-4 M2 (**5**) X = Cl, R = CH_3
DAF-FM (**6**) X = F, R = CH_3

Scheme 2.

3.4. Other NO sensors

Several other approaches to detecting NO, such as the use of small molecule sensors based on the reaction of rhodamine B hydrazine (RBH) with nitrite [97] or of dichlorodihydrofluorescein and dihydrorhodamine with a number of oxidants [98–101], have problems similar to those encountered in the application of DAFs. One possible solution to developing a sensor with the ability to bind NO selectively and reversibly is to use the formation of a transition metal nitrosyl as the signaling methodology. Such an approach would provide accurate concentration estimates by effectively competing with superoxide and metalloenzymes for NO, and eliminating misleading signals from RNOS species. Recently a quinoline pendant cyclam sensor that mimics the structure and activity of sGC has been used as a fluorescent NO sensor [102]. In the absence of NO, the quinoline fluorophore is coordinated to the Fe^{2+} center similar to the distal histidine of sGC. In the proposed mechanism, an Fe-nitrosyl is formed upon exposure to NO under anerobic conditions, and the quinoline fluorophore is released (Scheme 3). The release of the quinoline results in a fluorescence decrease. Although the quinoline pendent cyclam sensor monitors NO by fluorescence quenching, a pH sensor that utilizes a similar strategy with a Ni^{2+} cyclam produces a positive response [103].

3.5. Co tropocoronand complexes

During the course of research in our laboratory on the reactivity of Fe [104], Mn [105] and Co [106–108] tropocoronand complexes, we reasoned that the related aminotroponiminate ligands might be amenable to the development of Co(II)-based fluorescent NO sensors. A procedure for synthesizing *N*,*N*′-disubstituted aminotroponimine (HR_2ATI) ligands was modified to produce a series of differentially substituted derivatives incorporating a dansyl (5-dimethylaminonaphthalenesulfonamide) fluorophore with either an isopropyl, *tert*-butyl or benzyl group (Scheme 4) [109]. The four-step synthetic route provided multi-gram quantities of the desired H^RDATI ligands in 20–50% yields. The Co(II) complexes formed by reacting 2 equiv. of the ligand with potassium or sodium hydride and $CoCl_2$ are air stable crystalline solids that are sensitive to moisture only in solution.

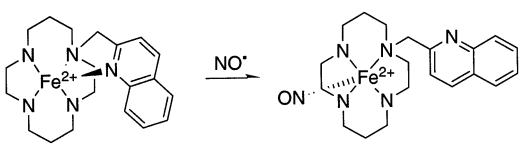

Scheme 3.

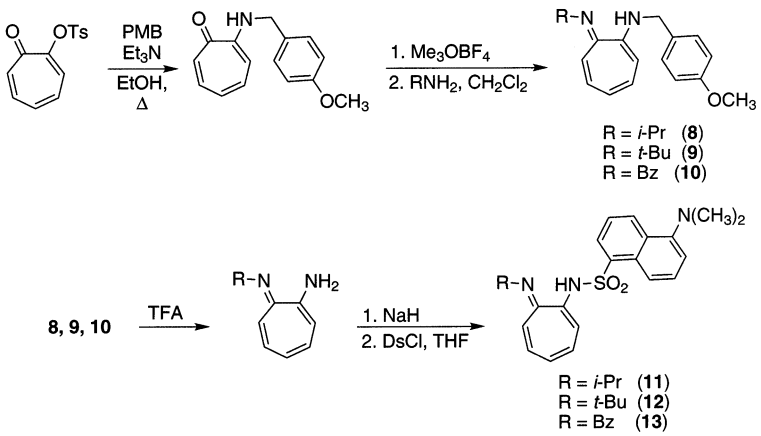

Scheme 4.

X-ray structural studies of [Co($^{i\text{Pr}}$DATI)$_2$] (**14**), [Co($^{t\text{Bu}}$DATI)$_2$] (**15**) and [Co($^{\text{Bz}}$DATI)$_2$] (**16**) revealed that the steric bulk of the ligand favors bis(chelate) four-coordinate Co^{2+} rather than tris(chelate) octahedral Co^{3+} complexes (Fig. 1) [110]. The Co center in **14** is pseudo-tetrahedral with a dihedral angle, Θ, of 76.1° between the two five-membered chelate rings. The differences in Θ for the *t*-butyl (81.4°) and benzyl (73.8°) derivatives reflect the different steric requirements of the ligands [109]. In addition, the dansyl groups of **16** are positioned with an appropriate orientation and the correct distance, 3.5(1) Å, for π–π stacking [111]. Although the coordination chemistry of Co sulfonamides is limited to a few examples of octahedral [112–114] and tetrahedral [115,116] complexes, the bond distances and angles are consistent with expected values.

The HR_2ATI ligands **11**–**13**, exhibit a broad fluorescence emission with a maximum around 500 nm when excited at 350 nm. The Co complexes **14**, **15** and **16** display dramatically diminished fluorescence emission compared to the corresponding free ligands. Fig. 2 shows the relative fluorescence intensities of **11** and **14**, measured at 40 μM in CH_2Cl_2. Transition metal ions, particularly those of the first row with unoccupied of partially filled d shells, can provide non-radiative relaxation pathways for the excited states of fluorophores by an energy- or electron-transfer mechanism [117,118].

After several hours of exposure to NO, two new bands develop in the IR spectra of **14**, **15** and **16** at 1838, 1760 cm^{-1}, 1833, 1760 cm^{-1}, and 1833, 1755 cm^{-1}, respectively. These absorption bands correspond to the symmetric and asymmetric stretching modes of metal dinitrosyl complexes found between 1750–1798 and 1820–1876 cm^{-1} [119–126]. A ^{1}H NMR experiment with **14** revealed that, upon exposure to NO, the paramagnetic resonances of **14** slowly disappear over a 4-day period, to be replaced by two sets of peaks corresponding to two separate

diamagnetic compounds. Further studies demonstrated that one set of peaks arises from the formation of a Co-dinitrosyl species with the other set coming from H$^{i\text{Pr}}$DATI liberated from the Co center (Eq. (1)).

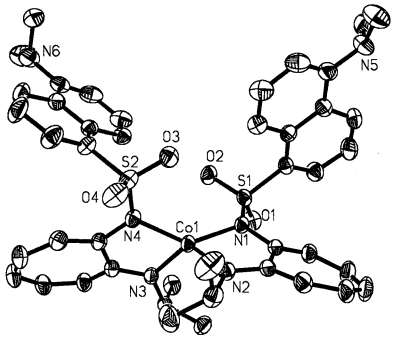

14

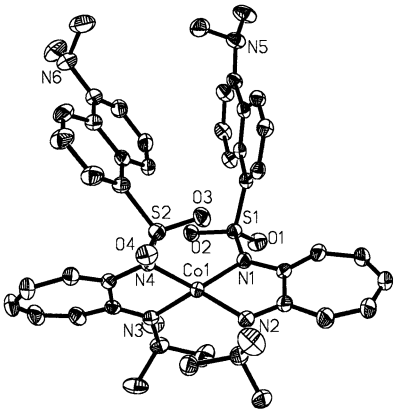

15

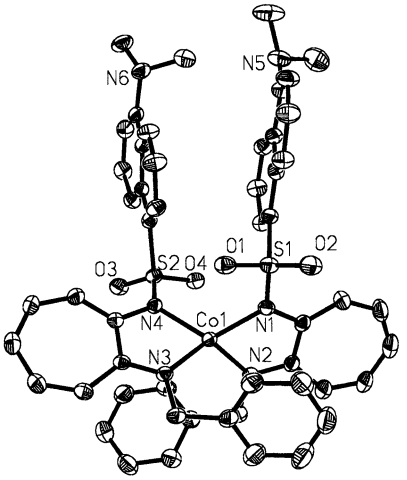

16

Fig. 1. ORTEP diagrams showing selected atom labels and 50% probability ellipsoids for all non-hydrogen atoms of [Co($^{i\text{Pr}}$DATI)$_2$] (**14**·CH_2Cl_2), [Co($^{t\text{Bu}}$DATI)$_2$] (**15**·CH_2Cl_2·THF), and [Co($^{\text{Bz}}$DATI)$_2$] (**16**·0.5 CH_2Cl_2·0.5 THF). Solvent molecules are omitted.

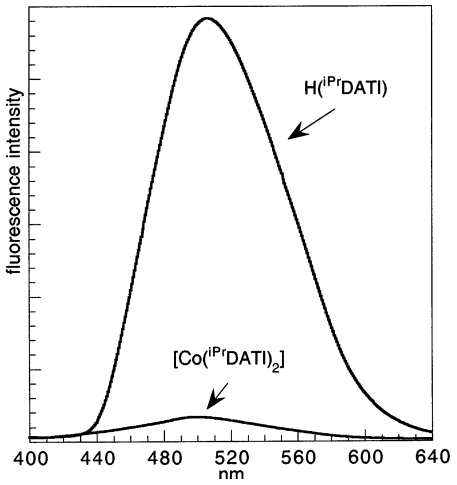

Fig. 2. Comparison of the fluorescence emission spectra of 46 μM CH_2Cl_2 solutions of H$^{i\mathrm{Pr}}$DATI and [Co($^{i\mathrm{Pr}}$DATI)$_2$] (**14**). Excitation = 350 nm.

$$[\mathrm{Co}(^{i\mathrm{Pr}}\mathrm{DATI})_2]\xrightarrow[\mathrm{e}^-,\,\mathrm{H}^+]{\mathrm{NO}^\bullet}[\mathrm{Co}(\mathrm{NO})_2(^{i\mathrm{Pr}}\mathrm{DATI})_2] + \mathrm{H}^{i\mathrm{Pr}}\mathrm{DATI} \quad (1)$$

14 **17**

The formation of the dinitrosyl complexes of **14**, **15** and **16** is accompanied by an intensity increase in fluorescence at 505 nm attributed to fluorescence from the liberated ligand fragment [109]. No fluorescence response occurs upon similar exposure of the complexes to O_2. The release of a ligand fragment as a signaling methodology led to the design DATI, an aminotroponimine that would remain coordinated after liberation of one of its dansyl components upon NO binding. The synthesis of H_2DATI-4 (**18**, Fig. 3) is similar to that of the unlinked ligands. The desired complex [Co(DATI-4)] (**19**) was readily obtained upon reaction of H_2DATI-4 with potassium hydride and $[Co(CH_3CN)_4](PF_6)_2$ [127]. The crystal structure of **19** revealed the Co^{2+} center to have a distorted tetrahedral geometry with $\Theta = 62.2°$ and the dansyl groups 3.63(9) Å apart, arranged in a π-stacking type of interaction (Fig. 4). The tetramethylene linker chain restricts the N2–Co1–N3

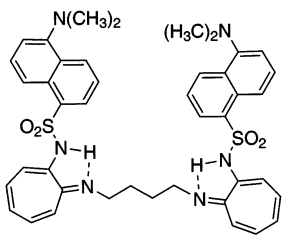

H_2DATI-4 (**18**)

Fig. 3. The linked tropocoronand ligand, H_2DATI-4 (**18**), prepared from a modified synthesis based on the unlinked compound preparation.

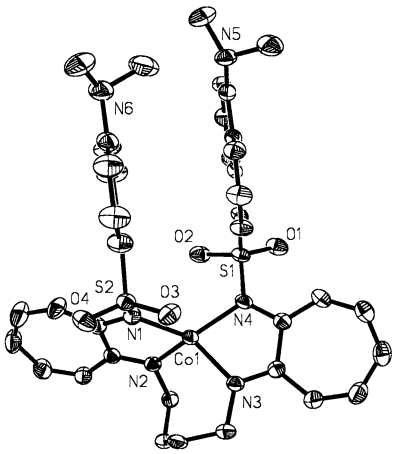

19

Fig. 4. ORTEP diagram of [Co(DATI-4)] (**19**) showing 50% thermal ellipsoids and selected atom labels.

angle to be 103.94(10)°, considerably smaller than the unrestricted N1–Co–N4 angle of 123.78(10)° on the opposite side of the complex.

One consequence of this geometry is that the reaction rate of **19** with NO is 50 times faster than $[Co(^{Bz}DATI)_2]$ and other analogs in which the dansylated aminotroponimiate moieties were not linked to one another. The distorted tetrahedral environment of **19** may permit better access of NO to the Co center, and the formation of the psuedotetrahedral dinitrosyl adduct may relieve geometric constraints in the starting complex, helping to drive the reaction. The formation of the desired dinitrosyl product was confirmed by the appearance of bands at 1835 and 1760 cm^{-1}, monitored by in situ IR spectroscopy. These peaks are analogous to those present in the unlinked compounds. NO stretching bands at 1827 and 1751 cm^{-1} in the solid state spectrum shift to 1793 and 1719 cm^{-1} following isotopic labeling experiments with ^{15}NO, in agreement with calculated values [109]. ^{1}H NMR experiments reveal the complex to be diamagnetic with proton resonances indicative of two types of ligand arm environments.

The fluorescence emission of the Co complex **19** ($\Phi = 9 \times 10^{-4}$) is dramatically quenched compared to that of the free ligand, **18** ($\Phi = 0.01$). Purging of the headspace over a 40 μM solution of **19** in CH_2Cl_2 with NO results in a doubling of the emission intensity at 505 nm ($\lambda_{ex} = 350$ nm) after 3 min; the intensity reaches a maximum 4-fold increase after 6 h (Fig. 5a). Similar exposure to air affords no such increase in fluorescence (Fig. 5b). Incremental addition of NO suggests the NO detection limit of **19** to be on the order of 50–100 μM.

The dissociation of a ligand arm from **19** to form the dinitrosyl cobalt complex removes one of the dansyl fluorophores from the quenching influence of the Co

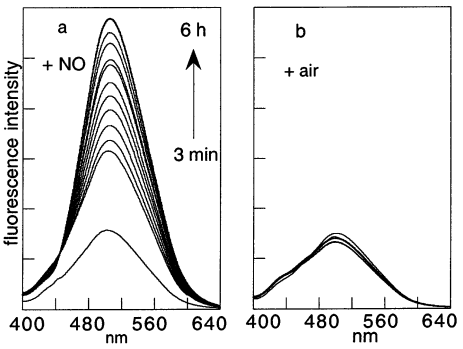

Fig. 5. (a) Fluorescence emission spectra showing the increase in intensity at 505 nm (excitation = 350 nm) when a 40 μM CH_2Cl_2 solution of [Co(DATI-4)] (**19**) was exposed to 1 atm NO gas. The lowest intensity spectrum is that of the starting material, the next spectrum was recorded 3 min after addition of NO into the headspace. After 6 h (top spectrum), a greater than fourfold increase in intensity over that of the starting material was observed. (b) The fluorescence emission spectra of 40 μM CH_2Cl_2 solution of **19** is unaffected by exposure to air over 6 h.

center and its ligands, which could account for the observed fluorescence increase (Scheme 5). In the Enemark–Feltham notation for nitrosyl compounds, the pseudo-tetrahedral cobalt dinitrosyl **20** is designated $\{Co(NO)_2\}^{10}$. The number of electrons, $n = 10$, in an $\{MNO\}^n$ complex corresponds to the sum of d-electrons of the metal and electrons in the π* orbitals of the NO ligands. The formation of such a diamagnetic cobalt dinitrosyl with a filled d^{10} shell may also remove a quenching mechanism and account for some of the fluorescence increase [127]. The π-stacking of the dansyl rings in the structure of **19** does not appear to be sufficient to induce eximer formation [128]; however, the radiative decay of the dansyl group involves a twisting of the dimethylamino group [129,130], and the proximity of two

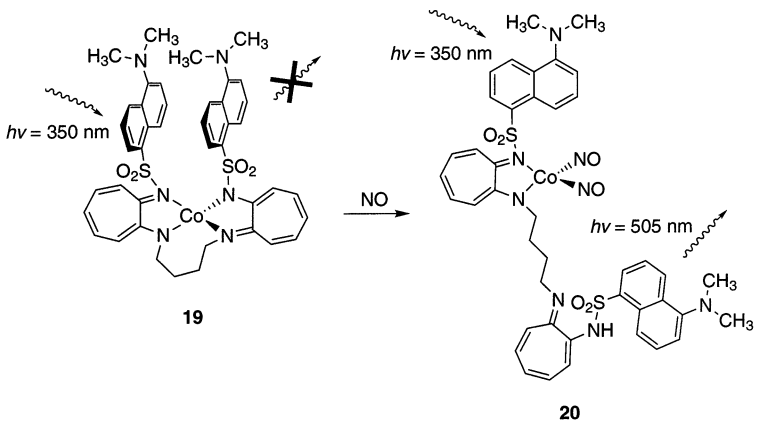

Scheme 5.

fluorophore rings in **19** may create a steric interaction that inhibits TICT (twisted internal charge transfer). Relaxation pathways involving unoccupied Co d-orbitals probably dominate the quenching mechanism.

The formation of a Co-dinitrosyl complex with fluorescent DATI ligands overcomes two important challenges for the detection of NO by small molecule sensors. It selectively reports NO over O_2 and generates a positive fluorescence response. Although the chemistry provides an important proof of principle, the current systems are unsuitable for intracellular applications because of their low sensitivity, water incompatibility, and irreversibility. Our current goals involve utilization of this new strategy for NO sensing to evolve probes for intracellular applications, specifically in neurobiology. Addressing the issues of reversible NO binding, water solubility, and better optical properties are the primary challenges.

4. Fluorescent sensors for Zn^{2+}

4.1. Zinquin and quinoline-based probes

Several strategies have been devised to detect Zn^{2+} by fluorescence including the use of peptides [131–133], proteins [134–136], and fluorophore-appended amines [137,138] and azamacrocycles [139–141]; however, none of these approaches are amenable to intracellular work [142]. The most widely used probes for detecting intracellular Zn^{2+} are the aryl sulfonamide derivatives of 8-aminoquinoline (Fig. 6), TSQ (**20**, 6-methoxy-(8-*p*-toluenesulfonamido)quino-line) [143], Zinquin (**21**) [144,145], and TFLZn (**22**) [146]. Recent investigations of the aqueous binding properties of these quinoline probes have clarified some discrepancies in the literature on these compounds [147]. Thermodynamic studies reveal that Zinquin analogues exhibit a high degree of cooperative binding to afford only the ZnL_2 complex under physiological conditions (Fig. 7). During Zn^{2+} binding the sulfonamide nitrogen becomes deprotonated, yielding a neutral complex that has been characterized by X-ray crystallography [148]. The fluorescence of these probes is independent of pH, and the intensity increases 100-fold by addition of excess Zn^{2+}, owing to metal coordination to the quinoline nitrogen atom, which inhibits a

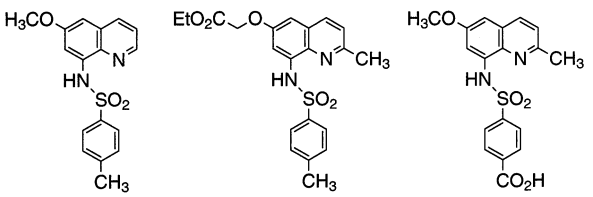

TSQ (**20**) Zinquin (**21**) TFLZn (**22**)

Fig. 6. The commonly employed quinoline-based fluorescent sensors for Zn^{2+} TSQ (**20**), Zinquin (**21**), and TFLZn (**22**).

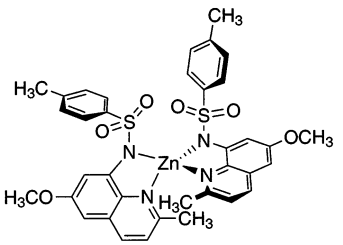

Fig. 7. Graphical representation of the X-ray crystal structure of the Zn^{2+} complex of a Zinquin derivative.

quenching pathway [148]. Zinquin can detect Zn^{2+} at 100 pM to 10 nM concentrations and has been used extensively to study intracellular Zn^{2+}. Vesicle-like punctate staining patterns are observed widely in a variety of eukaryotic cells, suggesting that the concentration of free Zn^{2+} exceeds 100 pM in such compartments [148]. Despite their ability to image intracellular Zn^{2+}, quinoline probes can form mixed complexes with partially coordinated Zn^{2+} in cells, generating uncertainty in measurements of free Zn^{2+}. In addition, quinoline probes have relatively dim fluorescence with quantum yields ca. 0.1 and extinction coefficients ca. 10×10^{-3} [149]. Moreover, their excitation wavelengths are somewhat shorter than desired, so there is considerable room for improvement in sensors to facilitate the study of intracellular Zn^{2+}.

4.2. Cyclen macrocycles

In one approach, macrocyclic amines were applied to prepare dansylamidoethylcyclen (**23**), a sensor capable of detecting Zn^{2+} at sub-nanomolar concentrations ($K_d = 5.5 \times 10^{-13}$) at physiological pH (Scheme 6) [150]. Like the quinoline sulfonamides, compound **23** has an excellent selectivity for Zn^{2+} over Mg^{2+} and Ca^{2+}, two major competing divalent cations present in cells, owing to the use of a sulfonamide ligand. Compound **23** has a low quantum yield in aqueous solution ($\Phi = 0.11$), however, exhibits only a fivefold fluorescence intensity enhancement, and has an excitation wavelength somewhat lower than optimal for intracellular work. The application of cyclen as a receptor for Zn^{2+} in a sensor was extended to a pair of probes utilizing xanthene chromophores as the reporting groups (Fig. 8) [151]. The two sensors ACF-1 (**24**) and ACF-2 (**25**) have excitation and emission wavelengths, $\lambda_{ex}/\lambda_{em} = 495/515$ and 505/525 respectively, in a range ideal for intracellular studies. At pH 7.5, the fluorescence intensity of **24** increases 14-fold upon saturation with Zn^{2+}, and **25** increases 26-fold. Although these sensors have exceptional optical properties, they have a fairly low affinity ($K_d \approx 5.7$ μM) [152], and require an intricate multi-step synthesis with low overall yields, 1.9% for **24** and 0.11% for **25**. Sensors **23**–**25** are presented as fluorescent probes for monitoring intracellular Zn^{2+}, but none has yet been employed successfully in biological studies.

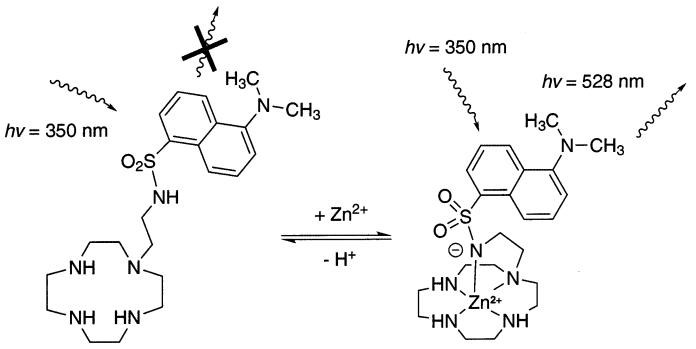

47

Scheme 6.

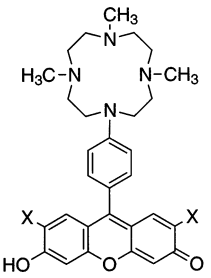

ACF-1, X = H (**24**)
ACF-2, X = Cl (**25**)

Fig. 8. Xanthene-based fluorescent sensor for Zn^{2+} that employs a cyclen macrocycle as the metal ion binding moiety.

4.3. Other Zn^{2+} sensors

Several other sensors have been used with varying degrees of success to study Zn^{2+} in biological systems. Newport Green (**26**), a 2′,7′-dichlorofluorescein-based sensor (Fig. 9), exhibits a 3.3-fold enhancement under physiological conditions, but has a relatively high dissociation constant ($K_d \approx 1$ μM) [149]. Traditional probes for Ca^{2+} and Mg^{2+} including fura-2 (**27**), mag-fura-2 (**28**), and mag-fura-5 (**29**) have been used as intracellular Zn^{2+} sensors (Fig. 10), but the Zn^{2+}-induced signals can be difficult to delineate from those from the alkali earth metal ions [51,153]. With such probes the concentrations of chelatable Zn^{2+} have been estimated to range from sub-nM in undifferentiated mammalian cells [148] to ca. 0.3 mM in hippocampal nerve synaptic vesicles [146]. In addition to its roles in the CNS and involve-

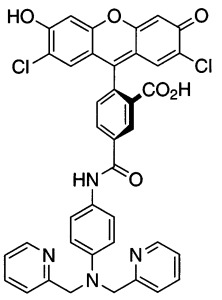

26

Fig. 9. The fluorescein-based fluorescent sensor for Zn^{2+} Newport Green (**26**).

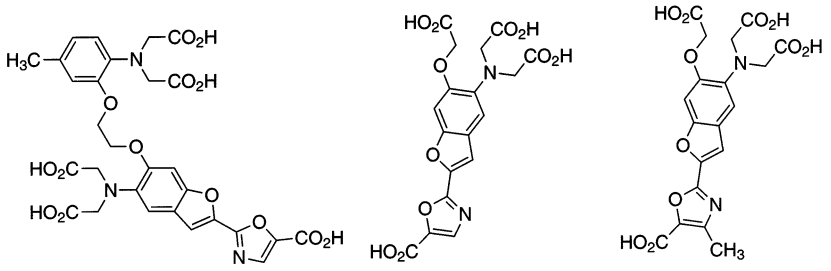

27 28 29

Fig. 10. Traditional Ca^{2+} sensor fura-2 (**27**), and Mg^{2+} sensors mag-fura-2 (**28**) and mag-fura-5 (**29**) that have been used as Zn^{2+} sensors.

ment in neurodegenerative disorders [37,38], zinc is a critical cofactor for numerous cellular functions [39], and is critical for gene expression [154] and apoptosis [144]. These many activities of Zn^{2+} suggest that it may be a major regulatory ion in the metabolism of cells [4,155]. With such a wide range of concentrations and functions, there is a need for improved probes for investigating Zn^{2+}.

4.4. Zinpyr sensors

We are interested in preparing Zn^{2+} sensors utilizing fluorescein as the chromophore. Fluorescein, a xanthene-based fluorophore, is well suited for sensor applications because of its high extinction coefficient, quantum yield approaching unity, membrane permeability, and the ready availability of optical filter sets for fluorescence microscopy. In order to achieve high affinity binding of Zn^{2+}, we chose to derivatize fluorescein with a DPA (di-2-picolylamine) fragment. This binding moiety is structurally similar to the high affinity, membrane permeant heavy metal chelator TPEN (*N*,*N*,*N*′,*N*′-tetra(2-picolyl)ethylenediamine) [156]. The $[Zn(DPA)]^{2+}$ complex has a K_d of 70 nM at pH 7, which may be compared to $[Zn(TPEN)]^{2+}$, for which K_d is 1 fM under similar conditions [157].

The derivatized fluorescein of interest was prepared by two different methodologies, each having its advantages. The ligand Zinpyr-1[1] (**30**, 9-(o-carboxyphenyl)-2,7-dichloro-4,5-bis[bis(2-pyridylmethyl)aminomethyl]-6-hydro-xyl-3-xanthenone) was synthesized in a Mannich reaction between 2′,7′-dichlorofluorescein (DCF) and the iminium ion condensation product of formaldehyde and DPA (Scheme 7) [158]. Under the Mannich conditions, reaction with fluorescein yields a mixture of structural isomers that cannot be separated by flash chromatography [159]. In an alternative synthesis, reductive amination of DPA with 4′,5′-fluoresceindicarboxaldehyde (**33**) yielded the closely related ligand Zinpyr-2 (**34**, 9-(*o*-carboxyphenyl)-4,5-bis[bis(2-pyridylmethyl)aminomethyl]-6-hydroxyl-3-xanthenone). The preparation of Zinpyr-2 involves derivatization of 4′,5′-dimethylfluorescein by a 4-step synthesis (Scheme 8).

Under simulated physiological conditions (50 mM PIPES (piperazine-*N*,*N*′-bis(2-ethanesulfonic acid)), 100 mM KCl, pH 7.0), Zinpyr-1 has an excitation maximum at 515 nm ($\varepsilon = 79.5 \times 10^3\ M^{-1}\ cm^{-1}$) and a quantum yield of 0.39 in the absence of Zn^{2+}. Addition of excess $ZnCl_2$ induces a slight blue shift in the excitation maximum (507 nm) and an increase in the quantum yield to 0.87. The emission maximum also shifts slightly upon Zn^{2+} addition, from 525 to 529 nm. Similarly, Zinpyr-2 has an excitation maximum at 498 nm ($\varepsilon = 36.7 \times 10^3\ M^{-1}\ cm^{-1}$) with a quantum yield of 0.25 that shifts to 490 nm accompanied by an increase in the quantum yield to 0.92 upon that addition of excess $ZnCl_2$. The emission maximum of free Zinpyr-2 is 518 nm and that of the Zn complex, 513 nm [160]. The fluorescence of unmetallated Zinpyr-1 and Zinpyr-2 is also pH-dependent with maximal emission occurring at pH 5.5 and almost complete quenching above pH 12. The pH-dependent fluorescence response could be fit to an apparent pK_a of 8.3 for Zinpyr-1 and 9.4 for Zinpyr-2. The Zn^{2+}-induced fluorescence enhancement is greater at high pH, consistent with quenching via PET from a deprotonated benzylic amine that is interrupted by coordination to Zn^{2+} [158]. The fluorescence of the Zinpyr dyes is responsive selectively to Zn^{2+} over other biologically relevant

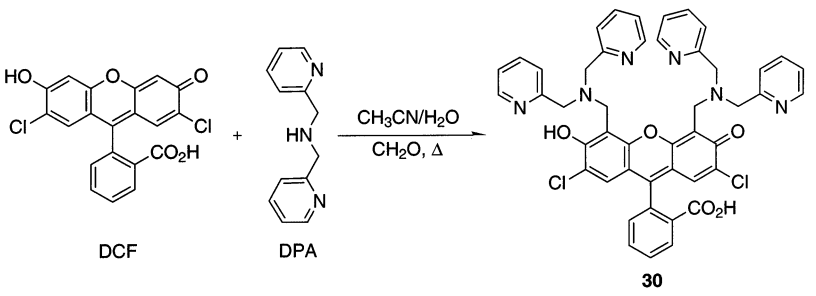

Scheme 7.

[1] The name Zinpyr indicates the structural composition of the ligand (four pyridyl groups) as well as its ability to 'peer' into the Zn^{2+} concentration of samples.

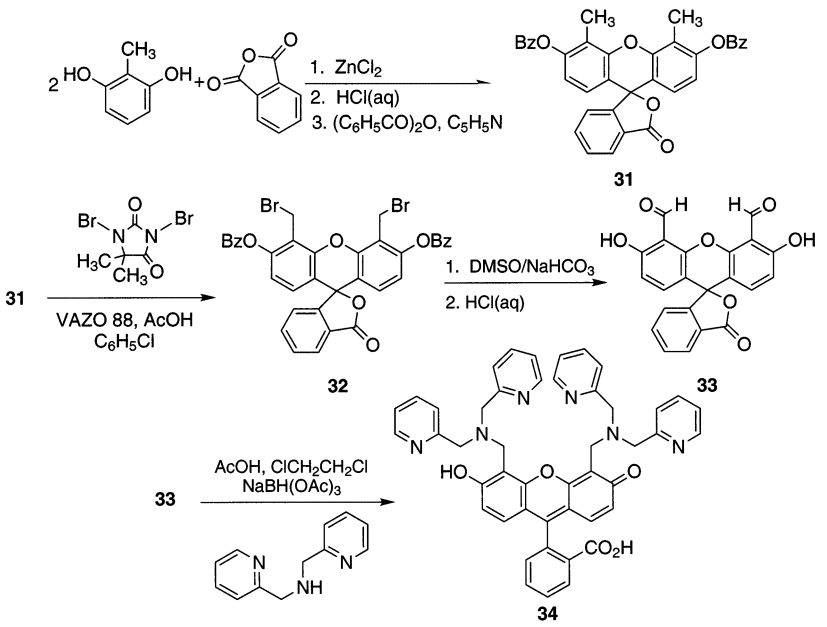

Scheme 8.

ions. The ions Mn^{2+}, Co^{2+}, Fe^{2+}, Ni^{2+}, and Cu^{2+} quench Zinpyr fluorescence, and Ca^{2+} and Mg^{2+} have a negligible effect on the intensity [158,160].

The metal ion affinity of the Zinpyr ligands was measured by a fluorescence titration experiment employing a dual-metal single-ligand buffer system [161] composed of 1 mM total EDTA, 2 mM Ca^{2+} (or Mg^{2+} up to 5 mM) and 0–1 mM total Zn^{2+}. The K_d of the $[Zn(EDTA)]^{2-}$ complex under these conditions is 2.11 nM, and the buffer system controls the variation of $[Zn^{2+}]$ and demonstrates the selectivity of the fluorescence response (Fig. 11). Although the quantum yield of Zinpyr-1 increases by 2.25-fold upon Zn^{2+} complexation, additional changes in the absorption of the ligand and metal complex induce a 3.1-fold increase in integrated emission with excitation at 507 nm. The quantum yield of Zinpyr-2 increases 3.7-fold and absorption changes produce an approximate sixfold increase in integrated intensity. The apparent K_d values of Zinpyr-1 and Zinpyr-2 were calculated to be 0.7 ± 0.1 and 0.5 ± 0.1 nM, respectively, with a Hill coefficient of 1 consistent with a 1:1 Zn^{2+}:ligand binding stoichiometry that is responsible for the intensity increase.

Binding of a second zinc ion is not accompanied by a fluorescence change, but can be measured by monitoring the absorption spectrum at higher concentrations of Zn^{2+}. Slight increases in absorption at 497 nm for Zinpyr-1 and at 486 nm for Zinpyr-2 at concentrations of Zn^{2+} exceeding 1 equiv. can be observed by meticulous measurements. At pH 7, Zinpyr-1 has a K_{d2} value of ca. 85 μM that drops to 35 μM at pH 7.5. The second binding event of Zinpyr-2 is accompanied

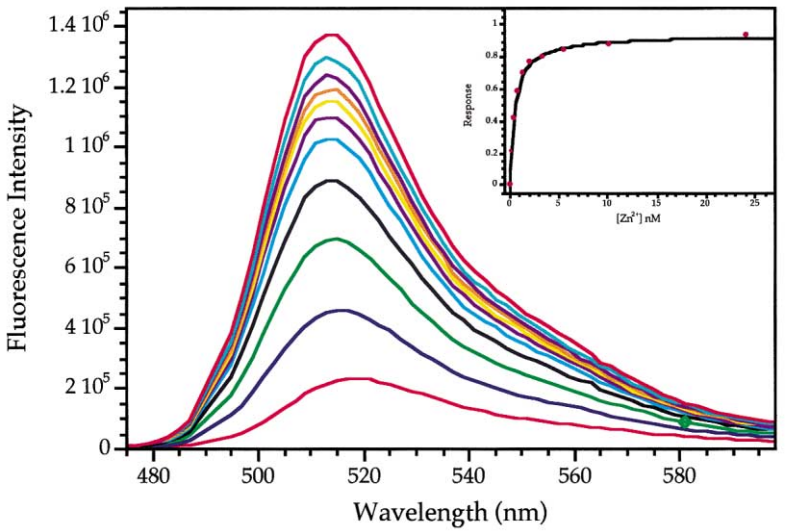

Fig. 11. Fluorescence emission response of Zinpyr-2 to buffered Zn^{2+} solutions. Spectra were acquired in 100 mM KCl, 50 mM PIPES, pH 7.00 at 25°C. Excitation was provided at 490 nm. The spectra correspond to buffered free zinc concentrations of 0, 0.172, 0.424, 0.787, 1.32, 2.11, 3.34, 5.60, 10.2 and 24.1 nM, respectively. The final spectrum is for $\sim$25 μM free Zn^{2+}. Inset: fitting curve obtained from the integration of the emission spectra from 500 to 575 nm after subtraction of the baseline (0 Zn^{2+}) and normalizing to the full scale response (25 μM free Zn^{2+}).

by changes in the absorption spectrum and fits to a K_{d2} of ca. 9 μM at pH 7, and ca. 2 μM at pH 7.5. The change in K_{d2} from pH 7 to 7.5 is consistent with the displacement of a proton from the ligand at the lower pH.

The nature of the zinc coordination environment in the Zn/Zinpyr complex was investigated by X-ray crystallography. In the structure of the perchlorate complex, two Zn^{2+} ions bind Zinpyr-1 (Fig. 12). Each Zn^{2+} is trigonal bipyramidal, coordinated by the three nitrogen donors of one DPA arm, a phenolic oxygen atom and a water molecule. The tertiary amines and water molecules are in the axial positions with the pyridine and phenol ligands occupying the equatorial sites. The crystal structure of $[Zn_2(\text{Zinpyr-1})(H_2O)_2(ClO_4)_2] \times x(H_2O)$ (**35**) is the first such determination of a fluorescein functionalized with metal-binding ligands.

Scheme 9 shows the expected solution coordination behavior of the Zinpyr ligands consistent with the physical measurements and X-ray structure. The modest fluorescence enhancement and pK_a values indicate that the benzylic amines responsible for PET quenching are largely protonated at physiological pH, and the correlation of the fluorescence enhancement with the binding of one Zn^{2+} suggests that the second benzylic amine is still protonated in the 1:1 Zn/Zinpyr complex. The large difference in K_d values for the two sites indicates different binding modes for the two Zn^{2+} ions, with the second site being coordinatively unsaturated. The closing of the lactone ring, which would not afford a fluorescent molecule, does not occur in aqueous solution and is probably the result of crystallization [160].

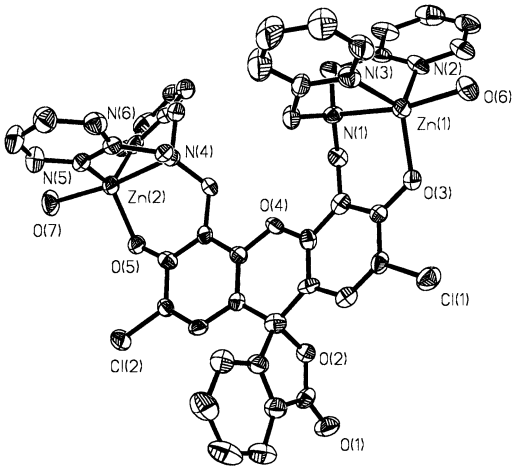

35

Fig. 12. ORTEP diagram of $[Zn_2(Zinpyr\text{-}1)(H_2O)_2(ClO_4)_2] \times x(H_2O)$ (**35**) showing 50% thermal ellipsoids and selected atom labels.

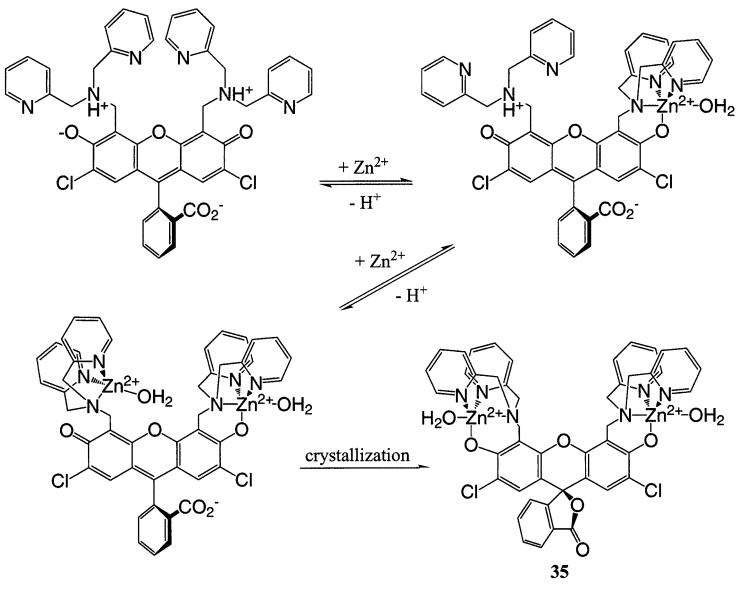

Scheme 9.

The capability of Zinpyr dyes to detect intracellular Zn^{2+} was demonstrated in Cos-7 cells labeled with 5 μM Zinpyr. Bright punctate staining that co-localized with the acidic-compartment probe LysoTracker (Molecular Probes, Eugene OR) occurred in a manner similar to observations made with quinoline-based sensors (Fig. 13a) [42,148]. Additional double-labeling experiments with a galactosyl transferase-enhanced cyan fluorescent protein fusion (GT-ECFP) that co-localizes in the medial/*trans*-Golgi [162] revealed that Zinpyr stains the Golgi or a Golgi-associated vesicle. An enhanced fluorescence was observed in the puncta after addition of exogenous Zn^{2+} with the zinc ionophore 2-mercapto-pyridine *N*-oxide (pyrithione Fig. 13b) that could be reversed by the addition of TPEN [158,160].

The primary shortcoming of the Zinpyr probes is their modest fluorescence enhancement at physiological pH. We are interested to extend and improve upon the chemistry developed during the course of our research to prepare future generation Zn^{2+} sensors with improved fluorescence behavior. Zinpyr is structurally similar to calcein (**36**), an early fluorescent sensor for Ca^{2+} (Fig. 14) [163]. Recently a sensor with elements of both calcein and Zinpyr, Zincarboxypyr-1 (**37**)[2],

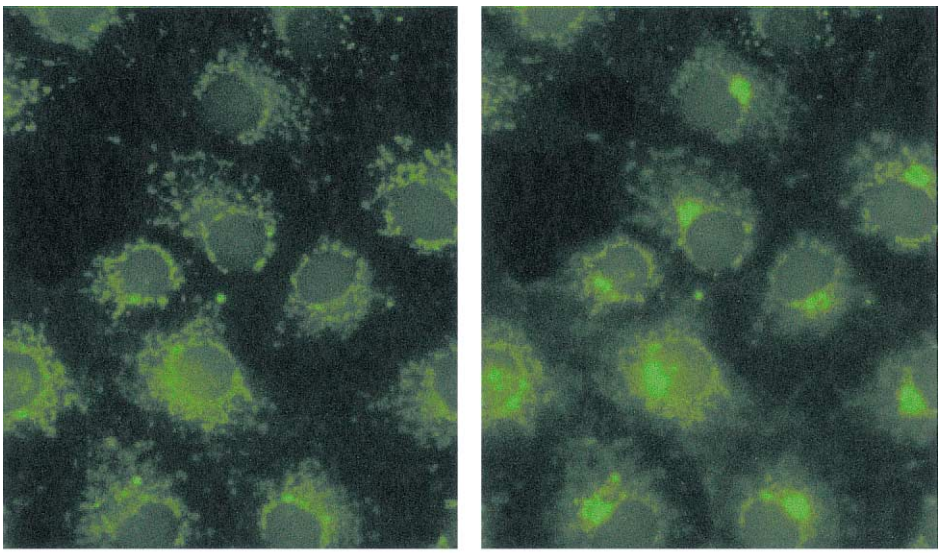

Fig. 13. (a) Fluorescence microscopy images of COS-7 cells labeled with 5 μM Zinpyr-1 for 0.5 h at 37°C. The fluorescence is not diminished by the addition of the high affinity membrane-permeable heavy-metal chelator, TPEN, indicating the fluorescence in not Zn^{2+}-induced. (b) The bright perinuclear punctate staining increases upon the addition of the zinc ionophore Zn^{2+}/pyrithione, and can be reversed by treatment with TPEN.

[2] The name Zincarboxypyr indicates the structural composition of the ligand two carboxylates and two pyridines.

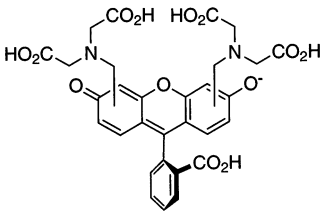

Calcein (**36**)

Fig. 14. The early fluorescein-based sensor for Ca^{2+}, calcein.

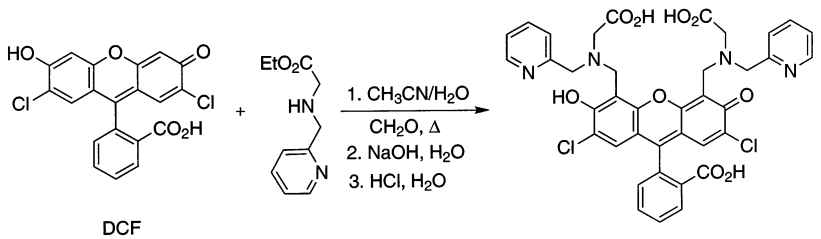

DCF

37

Scheme 10.

was synthesized in our laboratory by the Mannich reaction (Scheme 10). The introduction of a carboxylate donor further increased the pK_a value of the benzylic amine to 9.5, away from the desired range for use under physiological conditions [164]. Further experiments indicated that the Mannich reaction is too limited in scope to allow us to access the ligand families of interest. Our current objective is to prepare sensors that exhibit a greater fluorescence change upon metal binding with a single binding event.

5. Conclusions and future prospects

There have been numerous methodologies reported for detecting Ca^{2+}, Zn^{2+} and NO. We have devised a new strategy for sensing NO that produces a positive fluorescence change in response to the release of a fluorescent ligand arm from a Co center to form a metal–dinitrosyl complex. The [Co(DATI-4)] complex has relatively low affinity for NO (50–100 μM), but reacts specifically with NO and not O_2. An ideal NO biosensor should react reversibly with NO under aqueous, aerobic conditions, produce a more intense fluorescence response than we have achieved so far, and have different emission wavelengths in the bound and free states.

Our Zinpyr compounds have superior optical properties than other intracellular Zn^{2+} sensors owing to the use of fluorescein as the chromophore. A more dramatic change in emission intensity or wavelength is desirable, however, to measure zinc ion concentrations accurately. Initial investigations demonstrate the ability of our

fluorescein-based sensors to monitor Zn^{2+} in cells. We are continuing work with fluorescein scaffolds as a platform for preparing new and improved NO and Zn^{2+} sensors in an ongoing effort to study the roles of such species in neurotransmission.

A third focus of interest in our laboratory at the interface between coordination chemistry and the neurosciences is the potassium channel. In particular, we wish to construct small molecule mimics of the selectivity filter of the KcsA K^+ channel. Several approaches using calixarenes [165–167] and macrocycles [168] as models for ion channels have been reported, but they fail to mimic the key features of the K^+ channel structure. We are interested in building a model that more closely resembles the actual structure of the selectivity filter. In this ongoing model work we plan to study aspects of the selectivity filter and ion flow that are difficult to examine at the resolution currently available from the crystal structure determination.

Interest in the sub-field of metalloneuroscience is continuing to grow in the bioinorganic chemistry community [11]. The study of ion channels and pumps [17,19], transition metals in normal and disease states [13,31], brain enzymes like nerve growth factor [169] and synaptotagmin [170], and the continuing need for new and better sensors [67,68,142] highlight only some of the potential areas for future research. Understanding the inorganic chemistry of the brain will be vital to a full appreciation of memory formation, synaptic transmission, and neurodegenerative disorders in the new millennium.

Acknowledgements

The work in our laboratory that was reviewed in this article has been supported by the National Science Foundation, by seed money from MIT, and by a grant from the McKnight Foundation for the Neurosciences.

References

[1] S.J. Lippard, J.M. Berg, Principles of Bioinorganic Chemistry, University Science Books, Mill Valley, 1994.
[2] I. Bertini, H.B. Gray, S.J. Lippard, J. Valentine, Bioinorganic Chemistry, University Science Books, Mill Valley, 1994.
[3] A.X. Trautwein, Bioinorganic Chemistry, Wiley–VCH, Weinheim, 1997.
[4] J.J.R. Frausto da Silva, R.J.P. Williams, The Biological Chemistry of the Elements: the Inorganic Chemistry of Life, Oxford University Press, Oxford, 1991.
[5] J.A. Cowan, Inorganic Biochemistry An introduction, 2nd edn., Wiley–VCH, New York, 1997.
[6] R.H. Holm, E.I. Solomon, Chem. Rev. 96 (1996) 2237.
[7] C. Orvig, M.J. Abrams, Chem. Rev. 99 (1999) 2201.
[8] Z. Guo, P.J. Sadler, Angew. Chem. Int. Ed. Engl. 38 (1999) 1512.
[9] A.J. Thomson, H.B. Gray, Curr. Opin. Chem. Biol. 2 (1998) 155.
[10] J.S. Valentine, T.V. O'Halloran, Curr. Opin. Chem. Biol. 3 (1999) 129.
[11] S.J. Lippard, J.M. Berg, Curr. Opin. Chem. Biol. 4 (2000) 137.
[12] C.D. Garner, J. Chem. Soc. Dalton Trans. (1997) 3903.
[13] A.I. Bush, Curr. Opin. Chem. Biol. 4 (2000) 184.

[14] G.M. Shepherd, Neurobiology, Oxford University Press, Oxford, 1994.
[15] D.A. Doyle, J.M. Cabral, R.A. Pfuetzner, A. Kuo, J.M. Gulbis, S.L. Cohen, B.T. Chait, K. MacKinnon, Science 280 (1998) 69.
[16] D.A. Dougherty, H.A. Lester, Angew. Chem. Int. Ed. Engl. 37 (1998) 2329.
[17] C. Miller, Curr. Opin. Chem. Biol. 4 (2000) 148.
[18] J.C. Skou, Angew. Chem. Int. Ed. Engl. 37 (1998) 2320.
[19] E. Carafoli, M. Brini, Curr. Opin. Chem. Biol. 4 (2000) 152.
[20] E.C. Cooper, Proc. Nat. Acad. Sci. USA 96 (1999) 4759.
[21] F. Lehmann-Horn, K. Jurkat-Rott, Physiol. Rev. 79 (1999) 1317.
[22] M. Nelson, EMBO J. 18 (1999) 4361.
[23] M. Aschner, Environ. Res. Sect. A 80 (1999) 105.
[24] H.V. Aposhian, R.T. Ingersoll, E.B. Montgomery, Environ. Res. Sect. A 80 (1999) 96.
[25] Q.R. Smith, O. Rabin, E.G. Chikhale, in: J.R. Connor (Ed.), Metals and Oxidative Damage in Neurological Disorders, Plenum Press, New York, 1997, pp. 113–130.
[26] Y. Glinka, M. Gassen, M.B.H. Youdim, in: J.R. Connor (Ed.), Metals and Oxidative Damage in Neurological Disorders, Plenum Press, New York, 1997, pp. 1–22.
[27] J.R. Prohaska, in: J.R. Connor (Ed.), Metals and Oxidative Damage in Neurological Disorders, Plenum Press, New York, 1997, pp. 57–71.
[28] T.D. Rae, P.J. Schmidt, R.A. Pufahl, V.C. Culotta, T.V. O'Halloran, Science 284 (1999) 805.
[29] J.G. Joshi, in: J.R. Connor (Ed.), Metals and Oxidative Damage in Neurological Disorders, Plenum Press, New York, 1997, pp. 131–148.
[30] J.R. Connor, Metals and Oxidative Damage in Neurological Disorders, Plenum Press, New York, 1997.
[31] L.M. Sayre, G. Perry, M.A. Smith, Curr. Opin. Chem. Biol. 3 (1999) 220.
[32] C.J. Frederickson, Int. Rev. Neurobiol. 31 (1989) 145.
[33] E.P. Huang, Proc. Natl. Acad. Sci. USA 94 (1997) 13386.
[34] A.S. Prasad, in: J.R. Connor (Ed.), Metals and Oxidative Damage in Neurological Disorders, Plenum Press, New York, 1997, pp. 95–111.
[35] C.J. Frederickson, D.W. Moncrieff, Biol. Signals 3 (1994) 127.
[36] N.L. Harrison, S.J. Gibbons, Neuropharmacology 33 (1994) 935.
[37] D.W. Choi, J.Y. Koh, Ann. Rev. Neurosci. 21 (1998) 347.
[38] M.P. Cuajungco, G.J. Lees, Neurobiol. Dis. 4 (1997) 137.
[39] B.L. Vallee, K.H. Falchuk, Physiol. Rev. 73 (1993) 79.
[40] R.D. Palmiter, S.D. Findley, EMBO J. 14 (1995) 639.
[41] R.D. Palmiter, T.B. Cole, C.J. Quaife, S.D. Findley, Proc. Natl. Acad. Sci. USA 93 (1996) 14934.
[42] R.D. Palmiter, T.B. Cole, S.D. Findley, EMBO J. 15 (1996) 1784.
[43] M. Ebadi, Methods Enzymol. 205 (1991) 363.
[44] M. Ebadi, P.L. Iverson, R. Hao, D.R. Cerutis, P. Rojas, H.K. Happe, L.C. Murrin, R.F. Pfeiffer, Neurochem. Int. 27 (1995) 1.
[45] M. Ebadi, F. Perini, K. Mountjoy, J.S. Garvey, J. Neurochem. 66 (1996) 2121.
[46] R.D. Palmiter, S.D. Findley, T.E. Whitmore, D.M. Durnam, Proc. Natl. Acad. Sci. USA 89 (1992) 6333.
[47] D.L. Pountney, S.M. Fundel, P. Faller, N.E. Birchler, P. Hunziker, M. Vasak, FEBS Lett. 345 (1994) 193.
[48] S. Tsuji, H. Kobayashi, Y. Uchida, Y. Ihara, T. Miyatake, EMBO J. 11 (1992) 4843.
[49] Y. Uchida, K. Takio, K. Titani, Y. Ihara, M. Tomonaga, Neuron 7 (1991) 337.
[50] L. Slomianka, Neuroscience 48 (1992) 325.
[51] D. Atar, P.H. Backx, M.M. Appel, W.D. Gao, E. Marban, J. Biol. Chem. 270 (1995) 2473.
[52] J. Loscalzo, G. Welch, Prog. Cardiovasc. Dis. 38 (1995) 87.
[53] M.J. Rand, C.G. Li, Annu. Rev. Physiol. 57 (1995) 659.
[54] J. Garthwaite, C.L. Boulton, Annu. Rev. Physiol. 57 (1995) 683.
[55] H.M. Abu-Soud, D.J. Stuehr, Proc. Natl. Acad. Sci. USA 90 (1993) 10769.
[56] D.A. Dawson, in: J.R. Connor (Ed.), Metals and Oxidative Damage in Neurological Disorders, Plenum Press, New York, 1997, pp. 189–203.

[57] V.L. Dawson, T.M. Dawson, Neurochem. Int. 29 (1996) 97.
[58] F.T. Bonner, G. Stedman, in: M. Feelisch, J.S. Stamler (Eds.), Methods in Nitric Oxide Research, Wiley, New York, 1996, pp. 3–18.
[59] J.R. Lancaster, Nitric Oxide Biol. Chem. 1 (1997) 18.
[60] M.P. Doyle, J.W. Hoekstra, J. Inorg. Biochem. 14 (1981) 351.
[61] S. Pfeiffer, B. Mayer, B. Hemmens, Angew. Chem. Int. Ed. Engl. 38 (1999) 1714.
[62] E.M. Schuman, D.V. Madison, Science 263 (1994) 532.
[63] S. Tamir, S. Burney, S.R. Tannenbaum, Chem. Res. Toxicol. 9 (1996) 821.
[64] F. Laval, D.A. Wink, Carcinogenesis 15 (1994) 443.
[65] L.J. Ignarro, G.M. Buga, K.S. Wood, R.E. Byrns, G. Chaudhuri, Proc. Natl. Acad. Sci. USA 84 (1987) 9265.
[66] J.B. Schulz, R.T. Matthews, T. Klockgether, J. Dichgans, M.F. Beal, Mol. Cell. Biochem. 174 (1997) 193.
[67] A.W. Czarnik, Curr. Biol. 2 (1995) 423.
[68] A.P. de Silva, H.Q.N. Gunaratne, T. Gunnlaugsson, A.J. Huxley, C.P. McCoy, J.T. Rademacher, T.E. Rice, Chem. Rev. 97 (1997) 1515.
[69] R.Y. Tsien, Ann. Rev. Biophys. Bioeng. 12 (1983) 91.
[70] R.Y. Tsien, Trends Neurosci. 11 (1988) 419.
[71] R.Y. Tsien, Methods Cell Biol. 30 (1989) 127.
[72] R.Y. Tsien, Ann. Rev. Neurosci. 12 (1989) 227.
[73] R.Y. Tsien, T. Pozzan, Methods Enzymol. 172 (1989) 230.
[74] R.Y. Tsien, in: A.W. Czarnik (Ed.), Fluorescent Chemosensors for Ion and Molecule Recognition, vol. 538, American Chemical Society, Washington, DC, 1993, pp. 130–146.
[75] R.Y. Tsien, Chem. Eng. News 72 (1994) 34.
[76] J.B. Birks, Photophysics of Aromatic Molecules, Wiley–Interscience, London, 1970, pp. 492–517.
[77] S.A. Green, D.J. Simpson, G.P.S. Ho, N.V. Blough, J. Am. Chem. Soc. 112 (1990) 7337.
[78] H.H.H.W. Schmidt, M. Kelm, in: M. Feelisch, J.S. Stamler (Eds.), Methods in Nitric Oxide Research, Wiley, New York, 1996, pp. 491–497.
[79] T. Malinski, Z. Taha, S. Grunfeld, S. Patton, M. Kapturczak, P. Tomboulian, Biochem. Biophys. Res. Commun. 193 (1993) 1076.
[80] J.Y. Jin, T. Miwa, L.Q. Mao, H.P. Tu, J.T. Jin, Talanta 48 (1999) 1005.
[81] S. Trevin, F. Bedioui, J. Devynck, Talanta 43 (1996) 303.
[82] M. Feelisch, J.S. Stamler, Methods in nitric oxice research, in: M. Feelisch, J.S. Stamler (Eds.), Methods in Nitric Oxide Research, Wiley, New York, 1996, pp. 303–307.
[83] J.N. Abelson, M.I. Simon, Methods Enzymol. 268 (1996) 1.
[84] S.L.R. Barker, Y. Zhao, M.A. Marletta, R. Kopelman, Anal. Chem. 71 (1999) 2071.
[85] S.L.R. Barker, R. Kopelman, T.E. Meyer, M.A. Cusanovich, Anal. Chem. 70 (1998) 971.
[86] S.L.R. Barker, B.A. Thorsrud, R. Kopelman, Anal. Chem. 70 (1998) 100.
[87] S.L.R. Barker, R. Kopelman, Anal. Chem. 70 (1998) 4902.
[88] M. Batz, H.-G. Korth, R. Sustmann, Angew. Chem. Int. Ed. Engl. 36 (1997) 1501.
[89] M. Batz, H.-G. Korth, P. Meineke, R. Sustmann, Methods Enzymol. 301 (1999) 532.
[90] P. Meineke, U. Rauen, H. de Groot, H.-G. Korth, R. Sustmann, Chem. Eur. J. 5 (1999) 1738.
[91] R. Sustmann, Personal communication.
[92] H. Kojima, N. Nakatsubo, K. Kikuchi, S. Kawahara, Y. Kirino, H. Nagoshi, Y. Hirata, T. Nagano, Anal. Chem. 70 (1998) 2446.
[93] H. Kojima, Y. Urano, K. Kikuchi, T. Higuchi, Y. Hirata, T. Nagano, Angew. Chem. Int. Ed. Engl. 38 (1999) 3209.
[94] A.M. Miles, D.A. Wink, J.C. Cook, M.B. Grisham, Methods Enzymol. 268 (1996) 105.
[95] H. Kojima, K. Sakurai, K. Kikuchi, S. Kawahara, Y. Kirino, H. Nagoshi, Y. Hirata, T. Akaike, H. Maeda, T. Nagano, Biol. Pharm. Bull. 20 (1997) 1229.
[96] H. Kojima, M. Hirotani, Y. Urano, K. Kikuchi, T. Higuchi, T. Nagano, Tetrahedron Lett. 41 (2000) 69.
[97] T. Rieth, K. Sasamoto, Anal. Commun. 35 (1998) 195.

[98] K.M.K. Rao, J. Padmanabhan, D.L. Kilby, H.J. Cohen, M.S. Currie, J.B. Weinberg, J. Leukocyte Biol. 51 (1992) 496.
[99] P.G. Gunasekar, A.G. Kanthasamy, J.L. Borowitz, G.E. Isom, J. Neurosci. Methods 61 (1995) 15.
[100] J.P. Crow, Nitric Oxide 1 (1997) 145.
[101] A. Imrich, L. Kobzik, Nitric Oxide 1 (1997) 359.
[102] Y. Katayama, S. Takahashi, M. Maeda, Anal. Chim. Acta 365 (1998) 159.
[103] L. Fabbrizzi, M. Licchelli, P. Pallavicini, L. Parodi, Angew. Chem. Int. Ed. Engl. 37 (1998) 800.
[104] K.J. Franz, S.J. Lippard, J. Am. Chem. Soc. 121 (1999) 10504.
[105] K.J. Franz, S.J. Lippard, J. Am. Chem. Soc. 120 (1998) 9034.
[106] B.S. Jaynes, T. Ren, A. Masschelein, S.J. Lippard, J. Am. Chem. Soc. 115 (1993) 5589.
[107] B.S. Jaynes, L.H. Doerrer, S.C. Liu, S.J. Lippard, Inorg. Chem. 34 (1995) 5735.
[108] L.H. Doerrer, M.T. Bautista, S.J. Lippard, Inorg. Chem. 36 (1997) 3578.
[109] K.J. Franz, N. Singh, S.J. Lippard, Inorg. Chem. 39 (2000) 4081.
[110] F.A. Cotton, G. Wilkinson, Advanced Inorganic Chemistry, 5th edn., Wiley–Interscience, New York, 1988, pp. 724–741.
[111] Z.-H. Liu, C.Y. Duan, J. Hu, X.-Z. You, Inorg. Chem. 38 (1999) 1719.
[112] M. Borsari, L. Menabue, M. Saladini, J. Chem. Soc. Dalton Trans. (1996) 4201.
[113] S.Z. Haider, K.M.A. Malik, K.J. Ahmed, H. Hess, H. Riffel, M.B. Hursthouse, Inorg. Chim. Acta 72 (1983) 21.
[114] J.M. Castresana, M.P. Elizalde, J.M. Arrieta, G. Germain, J.-P. Declerq, Acta Crystallogr. Sect. C 40 (1984) 763.
[115] C.A. Otter, S.M. Couchman, J.C. Jeffery, K.L.V. Mann, E. Psillakis, M.D. Ward, Inorg. Chim. Acta 278 (1998) 178.
[116] V.E. Uhlig, M.Z. Doring, Anorg. Allg. Chem. 492 (1982) 52.
[117] R. Bergonzi, L. Fabrizzi, M. Licchelli, C. Mangano, Coordination Chem. Rev. 17 (1998) 31.
[118] L. Fabbrizzi, M. Licchelli, P. Pallavicini, Acc. Chem. Res. 32 (1999) 846.
[119] J.S. Field, P.J. Wheatley, S. Bhaduri, J. Chem. Soc. Dalton Trans. (1974) 74.
[120] B.L. Haymore, J.C. Huffman, N.E. Butler, Inorg. Chem. 22 (1983) 168.
[121] J.A. Kaduk, J.A. Ibers, Inorg. Chem. 16 (1977) 3283.
[122] B.E. Reichert, Acta Crystallogr. Sect. B 32 (1976) 1934.
[123] J.-L. Roustan, N. Ansari, Y. Le Page, J.-P. Charland, Can. J. Chem. 70 (1992) 1650.
[124] M. Aresta, D. Ballivet-Tkatchenko, M.C. Bonnet, R. Faure, H. Loiseleur, J. Am. Chem. Soc. 107 (1985) 2994.
[125] A.R. Hendrickson, R.K.Y. Ho, R.L. Martin, Inorg. Chem. 13 (1974) 1279.
[126] R.L. Martin, D. Taylor, Inorg. Chem. 15 (1976) 2970.
[127] K.J. Franz, N. Singh, S.J. Lippard, Angew. Chem. Int. Ed. Engl. 39 (2000) 2120.
[128] K.J. Franz, N.S. Singh, S.J. Lippard, Unpublished results.
[129] V. Balzani, F. Scandola, Supramolecular Photochemistry, Ellis Horwood, New York, 1991.
[130] J. Malkin, Photophysical and Photochemical Properties of Aromatic Compounds, CRC Press, Boca Raton, FL, 1992, pp. 123–127.
[131] H.A. Godwin, J.M. Berg, J. Am. Chem. Soc. 118 (1996) 6514.
[132] G.K. Walkup, B. Imperiali, J. Am. Chem. Soc. 119 (1997) 3443.
[133] G.K. Walkup, B. Imperiali, J. Org. Chem. 63 (1998) 6727.
[134] R.B. Thompson, M.W. Patchan, Anal. Biochem. 227 (1995) 123.
[135] D. Elbaum, S.K. Nair, M.W. Patchan, R.B. Thompson, D.W. Christianson, J. Am. Chem. Soc. 118 (1996) 8381.
[136] R.B. Thompson, B.P. Maliwal, Anal. Chem. 70 (1998) 1749.
[137] M.H. Huston, K.W. Haider, A.W. Czarnik, J. Am. Chem. Soc. 110 (1988) 4460.
[138] S.A. de Silva, A. Zavaleta, D.E. Baron, O. Allam, E.V. Isidor, N. Kashimura, J.M. Percarpio, Tetrahedron Lett. 38 (1997) 2237.
[139] E.U. AkkAya, M.H. Huston, A.W. Czarnik, J. Am. Chem. Soc. 112 (1990) 3590.
[140] A.W. Czarnik, Acc. Chem. Res. 27 (1994) 302.
[141] A. Bencini, M.A. Bernaro, A. Bianchi, V. Fusi, C. Giorgi, F. Pina, B. Valtanoli, Eur. J. Inorg. Chem. (1999) 1911.

[142] E. Kimura, T. Koike, Chem. Soc. Rev. 27 (1998) 179.
[143] C.J. Frederickson, E.J. Kasarskis, D. Ringo, R.E. Frederickson, J. Neurosci. Methods 20 (1987) 91.
[144] P.D. Zalewski, I.J. Forbes, W.H. Betts, Biochem. J. 296 (1993) 403.
[145] I.B. Mahadevan, M.C. Kimber, S.F. Lincoln, E.R.T. Tiekink, A.D. Ward, W.H. Betts, I.J. Forbes, P.D. Zalewski, Aust. J. Chem. 49 (1996) 561.
[146] T. Budde, A. Minta, J.A. White, A.R. Kay, Neuroscience 79 (1997) 347.
[147] C.J. Fahrni, T.V. O'Halloran, J. Am. Chem. Soc. 121 (1999) 11448.
[148] M.S. Nasir, C.J. Fahrni, D.A. Suhy, K.J. Kolodsick, C.P. Singer, T.V. O'Halloran, J. Biol. Inorg. Chem. 4 (1999) 775.
[149] R.P. Haugland, Handbook of Fluorescent Probes and Research Chemicals, 6th edn., Molecular Probes, Eugene, 1996, pp. 530–540.
[150] T. Koike, T. Watanabe, S. Aoki, E. Kimura, M. Shiro, J. Am. Chem. Soc. 118 (1996) 12696.
[151] T. Hirano, K. Kikuchi, Y. Urano, T. Higuchi, T. Nagano, Angew. Chem. Int. Ed. Engl. 39 (2000) 1052.
[152] G.K. Walkup, S.C. Burdette, Calculation based on fluorescence values reported in Ref. 149.
[153] L.M.T. Canzoniero, S.L. Sensi, D.W. Choi, Neurobiol. Dis. 4 (1997) 275.
[154] K.H. Falchuk, Mol. Cell. Biochem. 188 (1998) 41.
[155] T.V. O'Halloran, Science 261 (1993) 715.
[156] P. Arslan, F. Di Virgilio, M. Meltrame, R.Y. Tsien, T. Pozzan, J. Biol. Chem. 260 (1985) 2719.
[157] G. Anderegg, E. Hubmann, N.G. Podder, F. Wenk, Helv. Chim. Acta 60 (1977) 123.
[158] G.K. Walkup, S.C. Burdette, S.J. Lippard, R.Y. Tsien, J. Am. Chem Soc. 122 (2000) 5644.
[159] G.K. Walkup, R.Y. Tsien, unpublished results.
[160] S.C. Burdette, G.K. Walkup, B. Spingler, R.Y. Tsien, S.J. Lippard, J. Am. Chem. Soc. (2001) submitted for publication.
[161] H.U. Wolf, Experientia 29 (1973) 241.
[162] J. Llopis, J.M. McCaffery, A. Miyawaki, M.G. Farquhar, R.Y. Tsien, Proc. Natl. Acad. Sci. USA 95 (1998) 6803.
[163] H. Diehl, J.L. Ellingboe, Anal. Chem. 28 (1956) 882.
[164] C.W. Woodroofe, S.C. Burdette, S.J. Lippard, Unpublished results.
[165] P.J. Cragg, M.C. Allen, J.W. Steed, Chem. Comm. (1999) 553.
[166] J. De Mendoza, F. Cuevas, P. Prados, E.S. Meadows, G.W. Grokel, Angew. Chem. Int. Ed. Engl. 37 (1998) 1534.
[167] P. Schmitt, P.D. Beer, M.G.B. Drew, P.D. Sheen, Angew. Chem. Int. Ed. Engl. 36 (1997) 1840.
[168] C.D. Hall, G.J. Kirkovits, A.C. Hall, Chem. Comm. (1999) 1897.
[169] I.L. Shamovsky, G.M. Ross, R.J. Riopelle, D.F. Weaver, J. Am. Chem. Soc. 121 (1999) 9797.
[170] R.A. Garcia, C.E. Forde, H.A. Godwin, Proc. Nat. Acad. Sci. USA 97 (2000) 5883.